HHS Public Access

Author manuscript

Pediatr Res. Author manuscript; available in PMC 2013 November 01.

Published in final edited form as:

Pediatr Res. 2013 May ; 73(5): 661–667. doi:10.1038/pr.2013.29.

Single ventricle anatomy predicts delayed microstructural brain development

Viyeka Sethi[1], **Sarah Tabbutt**[1], **Anastasia Dimitropoulos**[2], **Kevin C. Harris**[2], **Vann Chau**[2], **Kenneth Poskitt**[3], **Andrew Campbell**[4], **Anthony Azakie**[5], **Duan Xu**[6], **Anthony J. Barkovich**[6], **Steven P. Miller**[1,2], and **Patrick S. McQuillen**[1]

[1]Department of Pediatrics, University of California, San Francisco Benioff Children's Hospital, San Francisco, CA

[2]Department of Pediatrics, University of British Columbia, British Columbia Children's Hospital, Vancouver, British Columbia, Canada

[3]Department of Radiology, University of British Columbia, British Columbia Children's Hospital, Vancouver, British Columbia, Canada

[4]Department of Surgery, University of British Columbia, British Columbia Children's Hospital, Vancouver, British Columbia, Canada

[5]Departments of Surgery, University of California, San Francisco Benioff Children's Hospital, San Francisco, CA

[6]Department of Radiology, University of California, San Francisco Benioff Children's Hospital, San Francisco, CA

Abstract

Background—Term newborns with congenital heart disease (CHD) show delayed brain development as early as the third trimester, especially in single ventricle physiology (SVP). Mechanisms causing delayed brain development in CHD are uncertain, but may include impaired fetal brain blood flow. Our objective was to determine if cardiac anatomy associated with obstruction to antegrade flow in the ascending aorta is predictive of delayed brain development measured by diffusion tensor imaging (DTI) and magnetic resonance spectroscopic imaging (MRSI).

Methods—Echocardiograms (ECHO) from 36 term newborns with SVP were reviewed for presence of aortic atresia and the diameter of the ascending aorta. Quantitative MR imaging parameters measuring brain microstructural (fractional anisotropy (FA), average diffusivity (Dav)) or metabolic development (N-acetylaspartate (NAA), Lactate/choline (Lac/cho)) were recorded.

Corresponding author: Patrick S. McQuillen, MD, 513 Parnassus Avenue, HSE 1421, San Francisco, CA 94143, Phone: 415-502-4798, Fax: 415-514-0235, McQuillP@peds.ucsf.edu.

DISCLOSURES: This study and study investigators have no disclosures, including no financial ties to products in the study or potential/perceived conflicts of interest.

Results—Increasing NAA/cho and white matter FA, and decreasing Dav and lactate/cho characterize normal brain development. Consistent with the hypothesis that delayed brain development is related to impaired brain perfusion, smaller ascending aortic diameter and aortic atresia were associated with higher Dav and lower white matter FA. ECHO variables were not associated with brain metabolic measures.

Conclusions—These observations support the hypothesis that obstruction to fetal cerebral blood flow impairs brain microstructural development.

INTRODUCTION

Adverse neurodevelopmental outcome is commonly noted in children with many forms of congenital heart disease (CHD) and the origins are pleiotropic. Acquired perioperative neurologic injury in the form of focal and diffuse white matter injury and small infarcts can be identified in the majority of infants with serious congenital heart disease requiring neonatal surgery (1–4). Thus, most efforts to improve neurodevelopmental outcome have focused on intraoperative care and cardiopulmonary bypass (5–9). Risk factors and mechanisms for these acquired brain injuries are incompletely described but speculated to include hypoxia, ischemia, inflammation and embolism (10, 11). Reported risk factors for post-operative brain injury on magnetic resonance imaging (MRI) include sustained and low regional cerebral oxygen saturation, low diastolic blood pressure and brain immaturity (1, 12, 13). Increasing evidence however, suggests that clinical and radiological neurologic abnormalities are present at birth (14) and may begin during fetal life (15).

MRI techniques have been developed to quantitatively measure aspects of brain development (16). For instance, diffusion tensor imaging (DTI) measures the direction and magnitude of water movement. With increasing brain microstructural development, the magnitude of brain water diffusion decreases and directionality increases, particularly in white matter. Structural axonal connectivity is maximal around birth and decreases postnatally. Analogous changes occur in metabolic compounds that can be measured by magnetic resonance spectroscopy (MRS). MRS measures brain metabolites, some of which exhibit distinct changes with development including increase in N-Acetylaspartate (NAA) and decrease in lactate (17). Use of these techniques, as well as measurement of brain volumes, have demonstrated that newborns with CHD have significant delays in brain development before surgery (18, 19). Onset of this delay in brain development occurs during the third trimester in utero (15). Delayed brain development could result from disruption of shared genetic or morphological developmental programs as many of the genes identified as causal for CHD also have important roles in brain development (20). A separate explanation arises from the observation that many forms of CHD affect fetal circulation to decrease brain oxygen or nutrient delivery, which might result in delayed brain development. Patients with hypoplastic left heart syndrome (HLHS) for example, have a spectrum of impairment to left ventricular ejection from complete aortic atresia, to mild aortic stenosis, that will variably influence the usual preferential streaming of oxygen and nutrient-rich placental blood antegrade through the aorta to the brain. This hypothesis suggests the testable prediction that postnatal echocardiographic parameters in patients with single ventricle physiology (SVP), suggestive of increased obstruction to antegrade flow to the head and

neck vessels, should be associated with greater magnitude of delayed brain development on quantitative MRI. Specifically, we hypothesize that increasing ascending aortic diameter or absence of aortic atresia, both indicative of more fetal antegrade flow, will be associated with less delay of microstructural and metabolic brain development.

RESULTS

Patient characteristics

There were 36 term infants (median gestational age 38.8 weeks), 18 male and 18 female, identified with single ventricle physiology. Their demographic data and postpartum characteristics are summarized in Table 1. Most of the infants were either prenatally diagnosed (N=22) or were diagnosed before developing shock or cardiac arrest due to closure of the ductus arteriosus. Thus, the score of neonatal acute physiology – perinatal extension (SNAP-PE), a validated illness severity and mortality risk score used in newborn intensive care patients (21), was not excessively high (median SNAP-PE 15). The lowest daily pre-operative oxygen saturation noted in the bedside flowsheet was 77±11%, indicating an expected degree of hypoxia. The majority of patients included had a diagnosis of HLHS (N=21) or variants of HLHS with aortic arch obstruction and required surgical palliation in the form of a Norwood procedure (summarized in Table 2). A smaller number of subjects (N=3) did not have arch obstruction and received varied surgical palliations. A total of 16 (43.2%) patients with aortic atresia were in the cohort.

Preoperative Brain Injury

Most patients had MRI performed in the first postnatal week (median day of life for preoperative MRI = 5 days, interquartile range 3 – 6 days). Brain injury was observed on the pre-operative MRI in 13 of 36 infants (36.1%), a similar percentage to that reported in other studies with larger populations and no restrictions on the type of CHD(1, 2, 22, 23). Brain injuries included mild white matter injury (WMI) in 4 (11.1%) patients, moderate in 4 (11.1%) and severe WMI in 2 of 36 newborns (5.5%). Focal strokes were noted in 6 of 36 patients (16.7%). All strokes were small, less than 1/3 of the vascular territory. Strokes occurred in middle (N=5) or posterior (N=1) cerebral artery territories. Intraventricular hemorrhages occurred in five patients (13.5%), 1 (2.7%) grade I and 4 (10.8%) grade II. No cases of global hypoxic ischemic injury were observed in this cohort.

Ascending aorta diameter and aortic atresia are associated with delay of microstructural but not metabolic brain development

The mean average diffusivity (Dav) for gray matter across all seven regions of interest (ROI) for our cohort was 1.17 ± 0.012 mm^2x10^{-3}/s and white matter was 1.52 ± 0.016 mm^2x10^{-3}/s. The mean fractional anisotropy (FA) in the white matter regions obtained in a similar fashion was 0.19 ± 0.004. This is a comparably higher Dav and lower white matter FA than previously published values for a cohort of healthy infants at term (24). Similarly, our cohort had comparably lower mean NAA/cho ratios (NAA/Cho = 0.566 ± 0.01) and higher mean Lac/cho ratios (Lac/cho = 0.142 ± 0.01) across all seven ROI's than previously published values for healthy neonates (24).

Aortic diameter for a normal 3.5-kg neonate is 9.3±0.9 mm (25). Aortic diameters for each CHD group and anatomical diagnosis are summarized in Table 2. To explore the effect of increasing aortic diameter on quantitative MR measurements, we plotted the diffusion variables, Dav and fractional anisotropy white matter (FAWM), as well as the spectroscopic variables, NAA/Cho and Lac/Cho against quartiles of ascending aortic diameter. We summarized the raw data by gray and white matter regions of interest. These plots demonstrate that Dav decreases with increasing ascending aortic diameter quartile (Figure 1A). Similarly, we see an increase in FA across each ascending aortic quartile or increasing diameter (Figure 1B). NAA/Cho and Lac/Cho did not show a consistent relationship with arch diameter quartile (data not shown).

We then tested the association of predictor and outcome variables using a linear regression for repeated measures, corrected for gestational age at the time of the MRI (Table 3). We found a significant inverse relationship between aortic diameter and Dav, in that, as the ascending aortic diameter increased the mean Dav across all ROI decreased ($p < 0.001$; Coefficient (Coeff.) −16.3; 95% CI −25.2 to −7.3). The converse association was seen with white matter FA and ascending aortic diameter. As the ascending aortic diameter increased, mean white matter fractional anisotropy increased across all ROI ($p<0.001$; Coeff. 5.4; 95% CI 2.4 to 8.3). The relationship was significant for both axial (Eigen vector 1) and radial (mean Eigen vector 2, 3; Table 4) measures of diffusivity, although the radial measure was more strongly associated. Subjects with aortic atresia exhibit the smallest aortic diameters (mean±s.d. 2.3 ± 0.6 mm). Given the absence of anterograde flow into the ascending aorta, we repeated this analysis dividing subjects into groups of atresia and quartiles of aortic diameter for the remaining subjects. Using linear regression, the identical results are found including a significant inverse relationship between group and mean Dav ($p<0.001$; Coeff. −18.5; 95% CI −32.7 to −4.4) as well as white matter FA ($p<0.001$; Coeff. 6.0; 95% CI 0.9 to 11.1). The spectroscopic variables show less consistent relationships with increasing ascending aortic diameter. The diameter of the ascending aorta did not predict a significant change in the spectroscopy variables NAA/cho ($p=0.814$; Coeff. 0.002; 95% CI −0.01 to 0.02) or Lac/cho ($p=0.145$; Coeff. 0.008; 95% CI −0.00 to 0.02). This lack of association did not change analyzing subjects categorically.

We also used linear regression for repeated measures while correcting for the gestational age at the time of the scan to analyze the relationship between the presence of aortic atresia and microstructural and metabolic brain delay. We found a statistically significant direct relationship between higher Dav in neonates with aortic atresia ($p<0.001$; Coeff. 72.6; 95% CI 37.6–107.6), consistent with microstructural brain immaturity in the setting of aortic atresia. Similarly, there was a significant inverse relationship between white matter FA and aortic atresia ($p=0.009$; Coeff. −18.5; 95% CI −32.3 to −4.7). Again, the relationship was significant for both axial and radial diffusivity, with a stronger association for the radial measure (Table 4). The presence of aortic atresia did not significantly predict differences in NAA/cho ($p=0.157$; Coeff. 0.032; 95% CI −0.01 to 0.08) or Lac/cho ($p=0.245$; Coeff. −0.019; 95% CI −0.05 to 0.01). This relationship held when the analysis was limited to either white matter or gray matter alone.

As described above we saw significant relationships between ascending aortic diameter or aortic atresia and diffusion variables in a pattern suggesting delayed microstructural brain development. To explore whether this overall effect was similar across each ROI, we plotted the percent change in Dav and FA across individual ROI in comparison with the overall effect (Figure 2A, B). We found the associations did not differ meaningfully across regions of interest for both Dav and FA, suggesting a widespread brain association.

Ascending aortic diameter and aortic atresia do not predict WMI

Preoperative WMI is observed frequently in newborns with single ventricle physiology. We tested the relationship between aortic diameter and/or aortic atresia and preoperative WMI. Using logistic regression, we found no significant relationship between smaller ascending aortic diameter and the presence of WMI ($p= 0.656$; coeff. = −0.08; 95% CI = −0.44 to 0.27). Using a chi-square test we found that the presence of aortic atresia was not significantly associated with the presence of WMI ($p= 0.360$).

DISCUSSION

By comparing measurements of cardiac anatomy with quantitative MR parameters of brain development, we have determined that aortic diameter and the presence of aortic atresia are significantly associated with microstructural white matter development in newborns with single ventricle physiology. Specifically, we found that aortic diameter and the presence of aortic atresia predict average diffusivity and white matter fractional anisotropy. Increasing aortic diameter was associated with lower average diffusivity and higher white matter fractional anisotropy, a pattern associated with more advanced brain maturity. During cardiovascular development, increasing blood flow is thought to be associated with increased size and development of many cardiovascular structures, including chambers, valves and major vessels. Smaller aortic diameter or aortic atresia is suggestive of a pattern of restricted left ventricular ejection and diminished flow in the ascending aorta to the head and neck vessels. Overall, this pattern is consistent with the hypothesis that diminished antegrade fetal cerebral blood flow, oxygen and nutrient delivery leads to delayed brain development.

Changes in brain magnetic resonance diffusion and spectroscopy measurements over normal fetal and postnatal development provide a simplistic model for analyzing alterations in microstructural and metabolic brain development in congenital heart disease. Further support for this paradigm comes from alternative approaches utilizing macroscopic features of brain development including size, volume, formation of gyri and sulci, myelination and disappearance of germinal matrix (18). Using both tools, newborns with CHD appear approximately one month immature in comparison to normal newborns. Relevance for this concept is further supported by observations that certain features (e.g. brain volumes) can normalize over time following repair of CHD (26). Clearly many features of brain development, including neuronal circuit and synapse formation, cannot be assessed by current MRI tools and thus brain structural and functional abnormalities may exist but not be detected by MRI.

In normal fetal circulation oxygenated blood with an oxygen saturation (O2Sat) ~80–85% is returned through the umbilical vein and ductus venosus via the hepatic circulation. Umbilical venous blood (O2Sat ~73%) is preferentially shunted across the foramen ovale to the left atrium to supply the developing fetal brain. In CHD, there is a spectrum of abnormal blood flow and mixing that may lead to diminished brain oxygen and nutrient delivery. The most severely affected are those with hypoplastic left heart syndrome (HLHS). In HLHS, there is impairment to left ventricular ejection, resulting in reversal of flow across the foramen ovale and complete mixing of oxygenated blood in the atrium. Left sided obstruction may further diminish antegrade flow of this lower saturated blood and in the most severe cases, the developing fetal brain is supplied in a retrograde fashion via the ductus arteriosus.

Infants with CHD have smaller head volumes compared to infants with structurally normal hearts and this is particularly apparent in infants with HLHS (27). Head growth slows in fetuses with HLHS during the third trimester (28). This might be related to restriction of flow through the aorta. In a retrospective study of 129 infants with HLHS, ascending and transverse aorta measurements and presence of aortic valve atresia/stenosis were tested as predictors of microcephaly within that population (29). Among these, only a smaller ascending aortic diameter significantly predicted the presence of microcephaly ($p = 0.034$). There was no association between microcephaly and aortic atresia. Additional factors associated with microcephaly identified in the study were interactions between anatomical restrictions to flow, cerebral vascular resistance, and cerebral blood flow.

The importance of antegrade flow is illustrated by recent evidence of its role in delayed brain development in third trimester fetuses. In a prospective study, brain volume and metabolism were compared in 55 infants with CHD and 50 controls (15). Infants with CHD had smaller brain volumes and lower NAA/cho ratios indicating abnormal metabolic brain development. Infants with HLHS and transposition of the great arteries (TGA) and had the lowest NAA/cho ratios and mild elevations of Lac/cho. Also, lack of flow through the ascending aorta was a significant independent predictor of a lower NAA/cho. The measures of antegrade flow and cerebral blood flow in these studies capture a fixed moment in time whereas the contributions to brain development are based on complex dynamic interactions between the cerebral vasculature, intracardiac flow and ventricular output.

Interestingly, there were no significant associations found between cardiac anatomical predictors and spectroscopy outcomes (NAA, lactate) in our cohort. A lack of association persisted even if spectroscopic variables were analyzed separately for white and grey matter regions. This is consistent with our previous findings in a mixed population (SVP & TGA), where lactate was not significantly elevated relative to controls (19). One possible explanation for the lack of associations for NAA, might relate to the prevalence of glial pathology observed in fetuses and newborns with CHD. NAA is predominantly a neuronal biomarker. The neuropathological sequelae of WMI is a failure of normal myelination (30) resulting from destruction of oligodendrocyte progenitors and a maturation arrest of the oligodendrocyte precursor pool (31). Importantly, increases in white matter fractional anisotropy coincide with immature oligodendrocyte progression and maturation (32). WMI is also associated with an increase of reactive astrocytes and activated microglia in both

premature newborns (33) and fetuses with congenital heart disease (28). The onset of pathology in fetuses with SVP overlaps a peak in the proliferation of vulnerable oligodendrocyte progenitors (34). Finally, in our study, changes in white matter FA were driven by larger changes in radial (Eigen vector 2,3), rather than longitudinal (Eigen vector 1) diffusion, consistent with a disturbance of myelination.

Our hypothesis that a static measurement of postnatal aortic diameter reflects the dynamic range of fetal cerebral blood flow is overly simplistic. An exception to this paradigm occurs in the condition of fetal aortic stenosis in which fetal left heart structures are normal sized at diagnosis, yet the systemic ventricle becomes progressively dysfunctional. A subset of these patients progresses to HLHS. In an effort to better identify candidates for fetal balloon aortic valvuloplasty, studies have identified important predictors of that transformation. Among those, the presence of retrograde flow in the transverse arch was found to predict the progression to HLHS with 100% sensitivity and specificity (35). The heterogeneous onset and severity of left sided obstructive lesions, their impact on left ventricular function and the downstream effects on antegrade cerebral bloodflow are difficult to quantify using current imaging technologies. More sensitive, dynamic measurements of fetal cerebral blood flow are needed in the setting of adequate ventricular mass and outflow tract but reduced ventricular function. Measurement of retrograde blood flow in the aorta might have improved our ability to identify this subset of patients and improved the association with MR measures of metabolic brain development in our cohort. However, in our population almost all patients had large patent ductus arteriosus, which interfered with assessment of retrograde flow in the transverse arch via Doppler flow.

We found significant relationships for the diffusion variables (Dav and white matter FA) and the ascending aortic diameter, as well as aortic atresia. Examining the regional variability of these observations, Dav is higher with smaller aortic diameter across all ROIs. However, with white matter FA, the effect is more heterogeneous, with the largest changes in the optic radiations and perirolandic white matter. One explanation for this observation relates to the timing of white matter myelination. White matter maturation occurs at variable rates and follows a set pattern (36–38). The usual course follows myelination in the cerebral peduncles and pons at birth, followed by the posterior limb of the internal capsule. The optic radiations and pyramidal tract motor fibers are among the first cortical regions to myelinate after birth and are actively myelinating at the time of the preoperative scan. Other regions, including, the anterior limb of the internal capsule, genu of the corpus callosum and finally the anterior, posterior and parietal white matter mature at later ages.

This study carries important limitations including the lack of comparison to a normal control group without CHD. Despite this limitation, we demonstrate a significant association between ascending aortic diameter and the presence of aortic atresia and MRI measures of microstructural brain development (Dav and white matter FA). Specifically, we found smaller ascending aorta diameters or the presence of aortic atresia predict a higher Dav and a lower white matter FA in single ventricle physiology. Our data implicates an important role for impaired antegrade cerebral blood flow in delayed microstructural brain development in newborns with CHD. Future studies will be necessary to determine if fetal interventions to improve cerebral blood flow also restore brain development and improve outcomes.

MATERIALS AND METHODS

Patients

Newborns with single ventricle physiology who were born at or transferred to British Columbia Children's Hospital in Vancouver (University of British Columbia, UBC) and University of California Benioff Children's Hospital, San Francisco (UCSF) were studied in an ongoing prospective cohort study. Single-ventricle physiology was defined as the absence of one of the two functioning ventricles where the heart function in series would be incompatible with life and palliative surgical intervention is required. Enrollment of patients began in 2001 at UCSF and in 2007 at UBC and continued through 2011 at both centers. Exclusion criteria included gestational age at birth <36 weeks; suspected congenital infection or suspected/confirmed genetic or malformation syndrome. A total of 147 patients were consented and enrolled between the two centers. From the overall cohort, all 36 infants with single ventricle physiology were included in this analysis (34 newborns at UCSF). Newborns were enrolled after their parents provided informed written consent. Once informed consent was obtained, brain MRI was performed prior to and following cardiac surgery.

Institutional committees on human research at both University of California in San Francisco and University of British Columbia approved the study protocol.

Echocardiography

Pre-operative echocardiograms (ECHO) were performed on all patients as part of routine clinical care. Measurements were made by a single pediatric cardiologist at each center (UCSF- ST, UBC - KCH) blinded to the neuroimaging results. Presence of aortic atresia and the size of the ascending aorta above the sinotubular junction were determined according to American Society of Echocardiography chamber quantification guidelines (39) as described - see (40) for a diagram of the position of aortic diameter measurement. Aortic atresia was defined as the absence of antegrade flow.

MRI Studies

Preoperative MRI studies were performed as soon as the baby could safely be transported to the MRI scanner with the use of a specialized MRI compatible isolette with a neonatal head coil. Studies at UCSF were performed with pharmacologic sedation as needed on a 1.5Tesla system (GE Healthcare Signa Echo-speed, Buckinghamshire, UK) and included: 4-mm thickness T1 weighted sagittal and axial spin echo, 4mm thickness dual-echo T2 weighted spin echo, 1.5-mm thickness coronal volumetric 3D gradient echo with radiofrequency spoiling images and a diffusion tensor sequence (TR, 7000 ms; TE, 99.5 milliseconds; 3-mm section thickness; no gap; 3 repetitions per image; with 18 x 36 cm Field of view and 128 x 256 acquisition matrix), acquiring axial images through the whole brain with an in-plane resolution of 1.4 x 1.4 mm^2. We acquired 7 images per axial section, including a T2-weighted reference image (b= 0 seconds/mm^2) and 6–15 diffusion- weighted images (b=700 seconds/mm^2) in noncollinear gradient directions. At UBC, MRI studies were carried out without pharmacologic sedation on a Siemens 1.5 Tesla Avanto using VB 13A software and included comparable imaging sequences to UCSF(23). No adverse events occurred during

this protocol. A neuroradiologist reviewed each MRI for focal, multifocal or global changes as described previously (20). White matter injury was classified as (3): mild (1–3 foci each <2mm), moderate (>3 foci or >2mm) or severe (>5% of white matter volume).

Three-dimensional Magnetic Resonance Spectroscopy imaging (MRSI)

MRS employed point resolved spectroscopy (PRESS) pulse sequence technique using repetition time of 1 second and echo time of 144 milliseconds to allow for multi-voxel imaging as described previously (19, 41). The spectra were analyzed using automated routines developed by our group with voxels centered on seven listed anatomic regions in the white and grey matter bilaterally: 1. Basal Ganglia, 2. Thalamus, 3. Optic Radiation, 4. Calcarine Region, 5. Corticospinal Tracts, 6. Posterior White Matter, 7. Frontal White Matter – see(19) for exact position of voxel locations. .Each voxel was reviewed by a neuroradiologist (UCSF – AJB, UBC – KJP) to ensure consistency of voxel placement and an adequate signal intensity to noise ratio. Peak-area ratios of lactate/choline (Lac/cho), lactate/N-Acetylaspartate (NAA) and NAA/choline were calculated. The values from the left and right hemispheres were averaged and a mean value was used for analysis. N-acetylaspartate (NAA) is a neuronal marker that increases as the brain matures. Lactate is a marker of anaerobic metabolism that is almost undetectable in brain parenchyma at birth in normal healthy term infants. NAA/cho and Lac/cho ratios have been previously shown to increase (NAA/cho) or decrease (Lac/cho) during brain development (17, 42).

DTI (Diffusion Tensor Imaging)

DTI was performed using a sequence optimized at each site for neonatal brain imaging (described in (19,41), and DTI data has been analyzed across both centers in other neonatal studies (43)). The diffusion tensor in this situation is an ellipsoid the size and form of which manifests the direction and amount of free water diffusion, as described by maximum, eigenvalues and corresponding eigenvectors of the tensor. Average diffusivity (Dav) describes the magnitude of water motion during the period it is examined by each excitation during the DTI sequence. Fractional anisotropy (FA) describes the degree of directionality of water motion; a value closer to zero describes isotropic diffusion (water molecules that move equally in all directions, whereas a value close to one describes diffusion predominantly in one direction. White matter is relatively anisotropic compared to gray matter. Dav was calculated for voxels in the same seven anatomic regions as MRS imaging and FA was calculated for the white matter regions.

Statistics

We compared our predictor variables (aortic arch diameter and presence of aortic atresia) with the unadjusted mean values for ratios of NAA and lactate to choline, average diffusivity and fractional anisotropy of white and grey matter. We used linear regression for repeated measures for this comparison while adjusting for gestational age at the time of the MRI. These models each included an interaction term for site (UCSF or UBC) by region of interest. The interaction term for site by region of interest allows for the MRSI and DTI values in each region to vary by site (UCSF or UBC) as study subjects were imaged in different MRI scanners at two medical centers.

Logistic regression was also used to evaluate whether ascending aortic diameter was predictive of WMI and chi-square analysis to evaluate whether aortic atresia was predictive of WMI. All variables were analyzed using Stata Software, version 12, using a p value <0.05 to determine statistical significance.

Acknowledgments

STATEMENT OF FINANCIAL SUPPORT: Study supported by National Institute of Neurological Disorders and Stroke at the U.S. National Institutes of Health (grant 1R01NS063876), Canadian Institutes of Health Research, and the March of Dimes (#6-FY2009-303). SPM is supported by a Canada Research Chair (Tier 2) and Michael Smith Foundation for Health Research Scholar award.

References

1. Andropoulos DB, Hunter JV, Nelson DP, et al. Brain immaturity is associated with brain injury before and after neonatal cardiac surgery with high-flow bypass and cerebral oxygenation monitoring. J Thorac Cardiovasc Surg. 2010; 139:543–556. [PubMed: 19909994]
2. Mahle WT, Tavani F, Zimmerman RA, et al. An MRI study of neurological injury before and after congenital heart surgery. Circulation. 2002; 106:I109–114. [PubMed: 12354718]
3. McQuillen PS, Hamrick SE, Perez MJ, et al. Balloon atrial septostomy is associated with preoperative stroke in neonates with transposition of the great arteries. Circulation. 2006; 113:280–285. [PubMed: 16401771]
4. McQuillen PS, Barkovich AJ, Hamrick SE, et al. Temporal and anatomic risk profile of brain injury with neonatal repair of congenital heart defects. Stroke. 2007; 38:736–741. [PubMed: 17261728]
5. Clancy RR, McGaurn SA, Goin JE, et al. Allopurinol neurocardiac protection trial in infants undergoing heart surgery using deep hypothermic circulatory arrest. Pediatrics. 2001; 108:61–70. [PubMed: 11433055]
6. du Plessis AJ, Jonas RA, Wypij D, et al. Perioperative effects of alpha-stat versus pH-stat strategies for deep hypothermic cardiopulmonary bypass in infants. J Thorac Cardiovasc Surg. 1997; 114:991–1000. discussion 1000–1001. [PubMed: 9434694]
7. Goldberg CS, Bove EL, Devaney EJ, et al. A randomized clinical trial of regional cerebral perfusion versus deep hypothermic circulatory arrest: outcomes for infants with functional single ventricle. J Thorac Cardiovasc Surg. 2007; 133:880–887. [PubMed: 17382619]
8. Jonas RA, Wypij D, Roth SJ, et al. The influence of hemodilution on outcome after hypothermic cardiopulmonary bypass: results of a randomized trial in infants. J Thorac Cardiovasc Surg. 2003; 126:1765–1774. [PubMed: 14688685]
9. Newburger JW, Jonas RA, Wernovsky G, et al. A comparison of the perioperative neurologic effects of hypothermic circulatory arrest versus low-flow cardiopulmonary bypass in infant heart surgery. N Engl J Med. 1993; 329:1057–1064. [PubMed: 8371727]
10. du Plessis AJ. Neurologic complications of cardiac disease in the newborn. Clin Perinatol. 1997; 24:807–826. [PubMed: 9395864]
11. Wernovsky G. Current insights regarding neurological and developmental abnormalities in children and young adults with complex congenital cardiac disease. Cardiol Young. 2006; 16 (Suppl 1):92–104. [PubMed: 16401370]
12. Dent CL, Spaeth JP, Jones BV, et al. Brain magnetic resonance imaging abnormalities after the Norwood procedure using regional cerebral perfusion. J Thorac Cardiovasc Surg. 2006; 131:190–197. [PubMed: 16399311]
13. Galli KK, Zimmerman RA, Jarvik GP, et al. Periventricular leukomalacia is common after neonatal cardiac surgery. J Thorac Cardiovasc Surg. 2004; 127:692–704. [PubMed: 15001897]
14. Limperopoulos C, Majnemer A, Shevell MI, Rosenblatt B, Rohlicek C, Tchervenkov C. Neurologic status of newborns with congenital heart defects before open heart surgery. Pediatrics. 1999; 103:402–408. [PubMed: 9925832]

15. Limperopoulos C, Tworetzky W, McElhinney DB, et al. Brain volume and metabolism in fetuses with congenital heart disease: evaluation with quantitative magnetic resonance imaging and spectroscopy. Circulation. 2010; 121:26–33. [PubMed: 20026783]
16. Huppi PS, Dubois J. Diffusion tensor imaging of brain development. Semin Fetal Neonatal Med. 2006; 11:489–497. [PubMed: 16962837]
17. Kreis R, Ernst T, Ross BD. Development of the human brain: in vivo quantification of metabolite and water content with proton magnetic resonance spectroscopy. Magn Reson Med. 1993; 30:424–437. [PubMed: 8255190]
18. Licht DJ, Shera DM, Clancy RR, et al. Brain maturation is delayed in infants with complex congenital heart defects. J Thorac Cardiovasc Surg. 2009; 137:529–536. discussion 536–527. [PubMed: 19258059]
19. Miller SP, McQuillen PS, Hamrick S, et al. Abnormal brain development in newborns with congenital heart disease. N Engl J Med. 2007; 357:1928–1938. [PubMed: 17989385]
20. McQuillen PS, Goff DA, Licht DJ. Effects of congenital heart disease on brain development. Prog Pediatr Cardiol. 2010; 29:79–85. [PubMed: 20802830]
21. Richardson DK, Phibbs CS, Gray JE, McCormick MC, Workman-Daniels K, Goldmann DA. Birth weight and illness severity: independent predictors of neonatal mortality. Pediatrics. 1993; 91:969–975. [PubMed: 8474818]
22. Beca J, Gunn J, Coleman L, et al. Pre-operative brain injury in newborn infants with transposition of the great arteries occurs at rates similar to other complex congenital heart disease and is not related to balloon atrial septostomy. J Am Coll Cardiol. 2009; 53:1807–1811. [PubMed: 19422989]
23. Block AJ, McQuillen PS, Chau V, et al. Clinically silent preoperative brain injuries do not worsen with surgery in neonates with congenital heart disease. J Thorac Cardiovasc Surg. 2010; 140:550–557. [PubMed: 20434174]
24. Bartha AI, Yap KR, Miller SP, et al. The normal neonatal brain: MR imaging, diffusion tensor imaging, and 3D MR spectroscopy in healthy term neonates. AJNR Am J Neuroradiol. 2007; 28:1015–1021. [PubMed: 17569948]
25. Kampmann C, Wiethoff CM, Wenzel A, et al. Normal values of M mode echocardiographic measurements of more than 2000 healthy infants and children in central Europe. Heart. 2000; 83:667–672. [PubMed: 10814626]
26. Ibuki K, Watanabe K, Yoshimura N, et al. The improvement of hypoxia correlates with neuroanatomic and developmental outcomes: comparison of midterm outcomes in infants with transposition of the great arteries or single-ventricle physiology. J Thorac Cardiovasc Surg. 2012; 143:1077–1085. [PubMed: 21963327]
27. Rosenthal GL. Patterns of prenatal growth among infants with cardiovascular malformations: possible fetal hemodynamic effects. Am J Epidemiol. 1996; 143:505–513. [PubMed: 8610666]
28. Hinton RB, Andelfinger G, Sekar P, et al. Prenatal head growth and white matter injury in hypoplastic left heart syndrome. Pediatr Res. 2008; 64:364–369. [PubMed: 18552707]
29. Shillingford AJ, Ittenbach RF, Marino BS, et al. Aortic morphometry and microcephaly in hypoplastic left heart syndrome. Cardiol Young. 2007; 17:189–195. [PubMed: 17338838]
30. Buser JR, Maire J, Riddle A, et al. Arrested preoligodendrocyte maturation contributes to myelination failure in premature infants. Ann Neurol. 2012; 71:93–109. [PubMed: 22275256]
31. Segovia KN, McClure M, Moravec M, et al. Arrested oligodendrocyte lineage maturation in chronic perinatal white matter injury. Ann Neurol. 2008; 63:520–530. [PubMed: 18393269]
32. Drobyshevsky A, Song SK, Gamkrelidze G, et al. Developmental changes in diffusion anisotropy coincide with immature oligodendrocyte progression and maturation of compound action potential. J Neurosci. 2005; 25:5988–5997. [PubMed: 15976088]
33. Back SA. Perinatal white matter injury: the changing spectrum of pathology and emerging insights into pathogenetic mechanisms. Ment Retard Dev Disabil Res Rev. 2006; 12:129–140. [PubMed: 16807910]
34. Back SA, Luo NL, Borenstein NS, Volpe JJ, Kinney HC. Arrested oligodendrocyte lineage progression during human cerebral white matter development: dissociation between the timing of

progenitor differentiation and myelinogenesis. J Neuropathol Exp Neurol. 2002; 61:197–211. [PubMed: 11853021]

35. Makikallio K, McElhinney DB, Levine JC, et al. Fetal aortic valve stenosis and the evolution of hypoplastic left heart syndrome: patient selection for fetal intervention. Circulation. 2006; 113:1401–1405. [PubMed: 16534003]
36. Barkovich AJ, Kjos BO, Jackson DE Jr, Norman D. Normal maturation of the neonatal and infant brain: MR imaging at 1.5 T. Radiology. 1988; 166:173–180. [PubMed: 3336675]
37. Brody BA, Kinney HC, Kloman AS, Gilles FH. Sequence of central nervous system myelination in human infancy. I. An autopsy study of myelination. J Neuropathol Exp Neurol. 1987; 46:283–301. [PubMed: 3559630]
38. Kinney HC, Brody BA, Kloman AS, Gilles FH. Sequence of central nervous system myelination in human infancy. II. Patterns of myelination in autopsied infants. J Neuropathol Exp Neurol. 1988; 47:217–234. [PubMed: 3367155]
39. Lang RM, Bierig M, Devereux RB, et al. Recommendations for chamber quantification: a report from the American Society of Echocardiography's Guidelines and Standards Committee and the Chamber Quantification Writing Group, developed in conjunction with the European Association of Echocardiography, a branch of the European Society of Cardiology. J Am Soc Echocardiogr. 2005; 18:1440–1463. [PubMed: 16376782]
40. Gautier M, Detaint D, Fermanian C, et al. Nomograms for aortic root diameters in children using two-dimensional echocardiography. Am J Cardiol. 2010; 105:888–894. [PubMed: 20211339]
41. Chau V, Poskitt KJ, McFadden DE, et al. Effect of chorioamnionitis on brain development and injury in premature newborns. Ann Neurol. 2009; 66:155–164. [PubMed: 19743455]
42. Glenn OA. Normal development of the fetal brain by MRI. Semin Perinatol. 2009; 33:208–219. [PubMed: 19631082]
43. Bonifacio SL, Glass HC, Chau V, et al. Extreme premature birth is not associated with impaired development of brain microstructure. J Pediatr. 2010; 157:726–732. e721. [PubMed: 20598316]

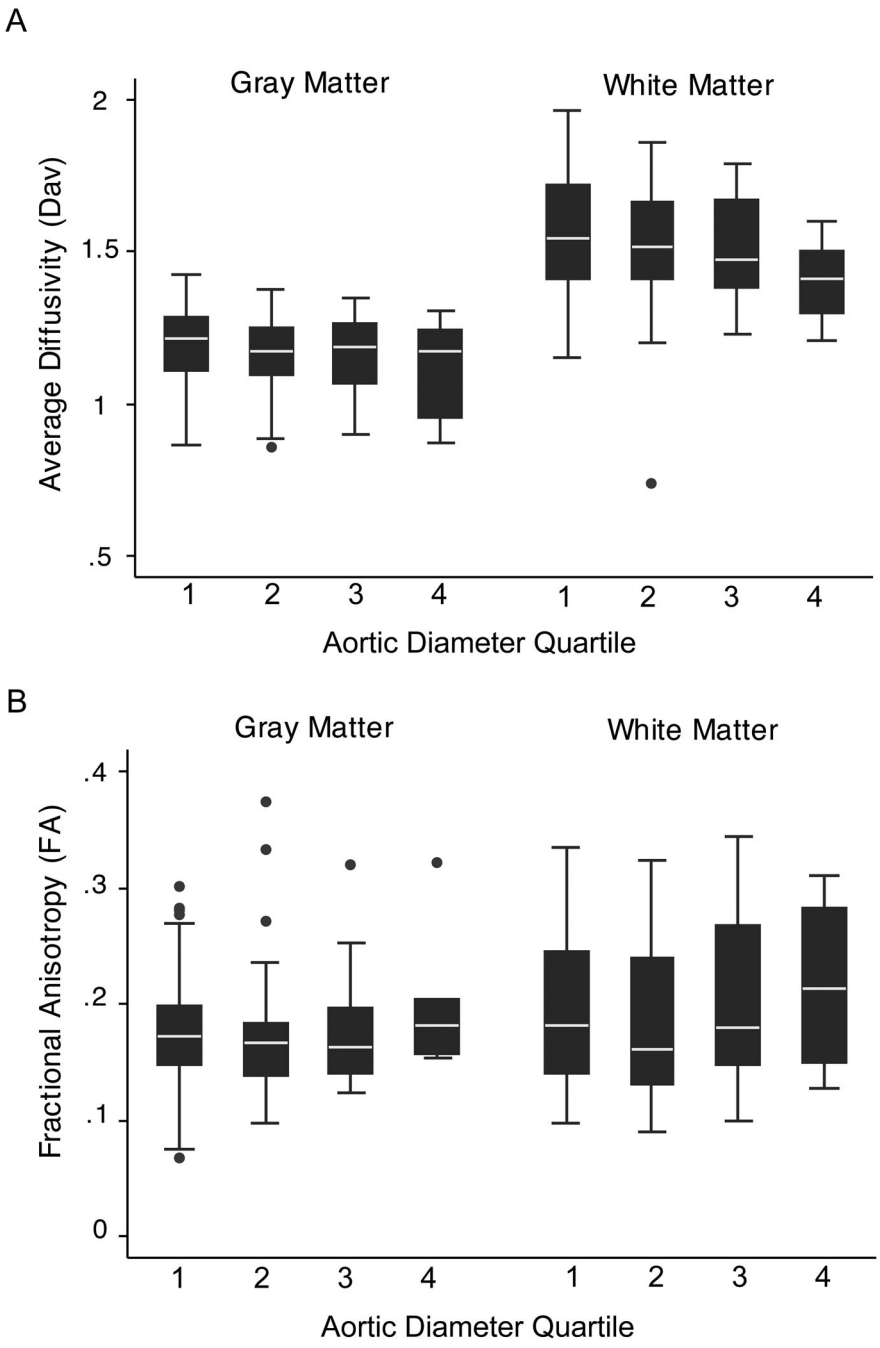

Figure 1.

Box and whisker plots of average diffusivity (Dav) (A) and fractional anisotropy (FA) (B) by arch quartile. Gray (basal ganglia, thalamus, calcarine cortex) and white matter (optic radiations, posterior, perirolandic and frontal white matter) regions of interest are averaged and plotted against quartiles of aortic diameter (1= 0–2.5 mm; 2= 2.6–5 mm; 3= 5.1–7.5 mm; 4= 7.6 – 10 mm). Each plot consists of the median – white line in the middle of the black box, the 25th and 75th percentiles – ends of black box, and the 5th and 95th percentile -- ends of the whiskers. Outliers are indicated by black circles.

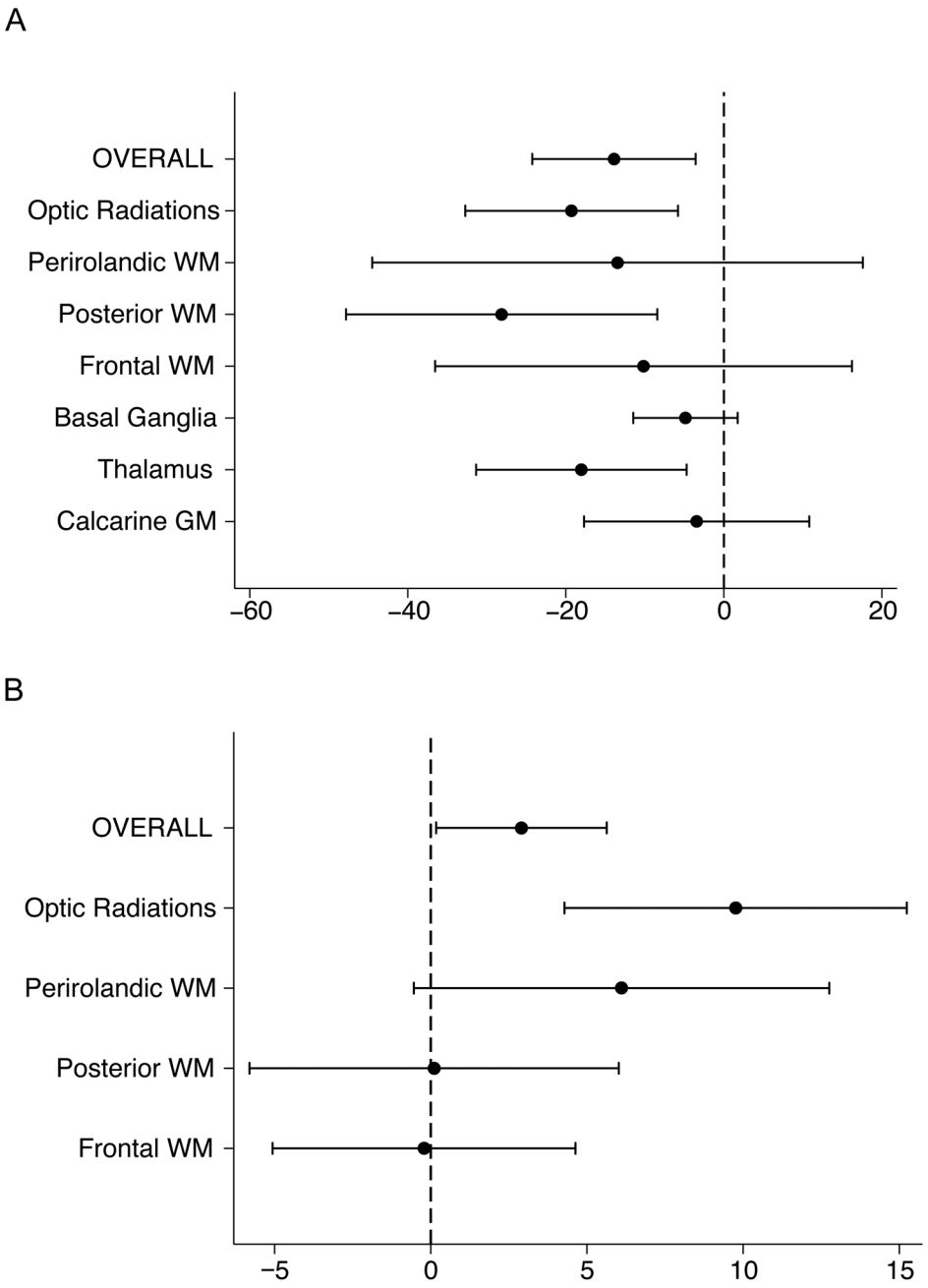

Figure 2.

Results of the regression analyses overall and by region of interest (ROI) for the association of average diffusivity (Dav) (a) and fractional anisotropy (FA) (b) with aortic diameter. Results are reported as the 95% confidence interval for percent difference of diffusion parameter per mm change in aortic diameter. WM, white matter; GM, gray matter.

Table 1

Clinical characteristics

Variable Mean ± SD Median (Range)	N=36
Male (%)	18 (52)
Birth weight (grams)	3185 ± 472
Birth head circumference (cm)	34 ± 1.4
Birth length (cm)	49 ± 6
Apgars @ 5 min	9 (5–9)
SNAP-PE	15 (10–59)
Gestational age at birth (weeks)	38.8 ± 1
Gestational age at MRI (weeks)	39.4 ± 1
MRI day	5 (1–13)
Preoperative Lowest O2 Sat	77 ± 11

SNAP-PE, Score of Neonatal Acute Physiology Perinatal Extension (27).

Table 2

Cardiac characteristics

Cardiac physiology	Cardiac Anatomy (N)	Aortic diameter (mean ±s.d.[a] mm)	Head Circumference (mean±sd cm)
SV[b] without arch obstruction (N=3)			
	SV[b] with PA[c] (2)	8.2 ± 1.5	37.5
	Unbalanced AVC[d] (1)	8.1	34
SV[b] with arch obstruction (N=33)			
	HLHS[e] with aortic atresia (16)	2.3 ± 0.6	34.3 ± 1.6
	HLHS[e] (6)	4.9 ± 0.9	34.7 ± 1.3
	TGA[f], SV[b] (4)	5 ± 1	33.7 ± 0.3
	Unbalanced AVC[d] (4)	5.2 ± 1.2	34.6 ± 1.4
	DORV[g] (3)	6.5 ± 0.9	34.3 ± 1.1

[a] s.d. – standard deviation;

[b] SV- single ventricle;

[c] PA- pulmonary atresia;

[d] AVC-atrioventricular canal;

[e] HLHS- hypoplastic left ventricle;

[f] TGA- transposition of great arteries;

[g] DORV- double outlet right ventricle;

Table 3

Results: echocardiographic and quantitative diffusion and spectroscopy variables

Predictor variable	Outcome variables	Coeff.	P-value	95% CI
Ascending aortic diameter	Dav[a]	−16.25	<0.001	−25.21 to −7.30
	FA[b] white matter	5.35	<0.001	2.40 to 8.30
	Eigen Vector 1	−18.58	0.005	−33.66 to −3.50
	Eigen Vector 2–3 (mean)	−25.55	<0.001	−38.92to −12.19
Aortic atresia	Dav[a]	72.65	<0.001	37.68 to 107.61
	FA[b] white matter	−18.51	0.009	−32.30 to −4.72
	Eigen Vector 1	90.36	0.005	27.70 to 153.04
	Eigen Vector 2–3 (mean)	108.54	<0.001	48.33 to 168.76

[a] Dav- average diffusivity;

[b] FA- fractional anisotropy